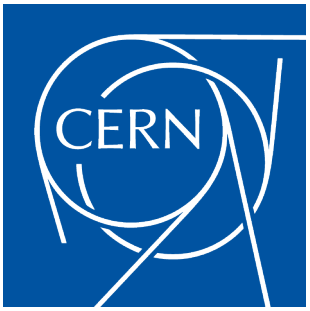

ÉCOLE POLYTECHNIQUE
FÉDÉRALE DE LAUSANNE

Computation of Linear Optics Distortions due to Head-on Beam-Beam Interactions in Hadron Colliders

Author : Patrik Gonçalves Jorge
Supervisor : Xavier Buffat

December 24, 2015

Computation of Linear Optics Distortions due to Head-on Beam-Beam Interactions in Hadron Colliders

Patrik Gonçalves Jorge

December 24, 2015

Contents

1 Introduction

1.1 General considerations and aims

A collider is a type of particle accelerator where two counter-rotating beams of particles collide head-on. The principal aim of this kind of accelerator is the study of basic constituents of matter : the fundamental particles. At CERN, the particles are made to collide together with a velocity very close to the one of the light so that they are high energetic (7 TeV for each beam). The purpose of such energy is the will to achieve new physics.

In this perspective, another criterion is important : the brightness of the beam. Indeed, the latter should be high which means that it is necessary to have a high intensity and a small beam size. These conditions are the key to high luminosity $\mathcal{L}$:

$$\mathcal{L} = f\frac{n_1 n_2}{n_b A} \tag{1}$$

where n_1 and n_2 are the total number of particles in each beam, f the revolution frequency, n_b the number of bunches in each beam and A characterize the cross section of the beams.

Each interaction between the beams will change the beam dynamics and therefore alter the beam envelope $\sigma = \sqrt{\beta\epsilon_g}$ where ϵ_g stands for the geometric emittance of the beam.

Indeed, since each beam is composed of moving bunches of charged particles, it implies that an electromagnetic field is induced by these ensembles of charges. This electromagnetic field will then affect the bunch itself and the other beam travelling in the opposite direction because of the forces acting on the charged particles. Note that the forces on the bunch itself, called space-charge forces, won't be taken into account afterwards since we are dealing with high-energy colliders ($\gamma \gg 1$) and that the force is proportional to $1/\gamma^2$, leading to a negligible effect.

The problem is that the particles constituting the beams may contact the elements of the accelerator after some perturbations and given the amount of energy of these particles, non negligible damages to the electronics and to the supraconducting magnets could be caused.

The solution to this issue is given by a system of collimators, whose aim is to protect the delicate elements of the machine, to help reduce the total dose on the accelerator equipment and to optimize the background for the experiments. It ensures in particular that the beam losses in superconducting magnets remain below quench limits. In order to clean the beams, specific insertions are dedicated to this function. This cleaning stage is achieved by placing very precisely blocks of materials close to the circulating beams, while respecting a pre-defined collimator hierarchy that ensures optimum cleaning in a multi-stage collimation process : primary and secondary collimators are the devices closest to the circulating beam, then come the shower absorbers and tertiary collimators that stand at larger apertures. The collimation hierarchy and therefore the cleaning efficiency is very sensitive to the machine optics, in particular to the β-function and the phase advance

between collimators.

Computer simulations with MAD-X program will be used to determine the optics variations due to one or several beam-beam interactions, i.e. the perturbations of the beams as they cross the opposing beam. What follows will treat more specifically the linear effects of head-on collisions. The simulation results will then be compared to theoretical expectations.

1.2 Accelerators studied

This report will focus on two different accelerators : the Future Circular Hadron-Hadron Collider (FCC-hh) and the High Luminosity Large Hadron Collider (HL-LHC). Their general layout and the name of their interaction points are presented in Fig. 1 and 2.

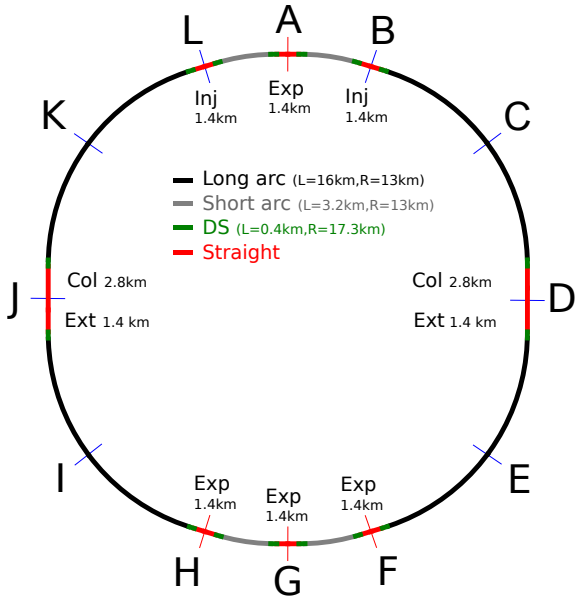

Figure 1: Layout of the FCC-hh

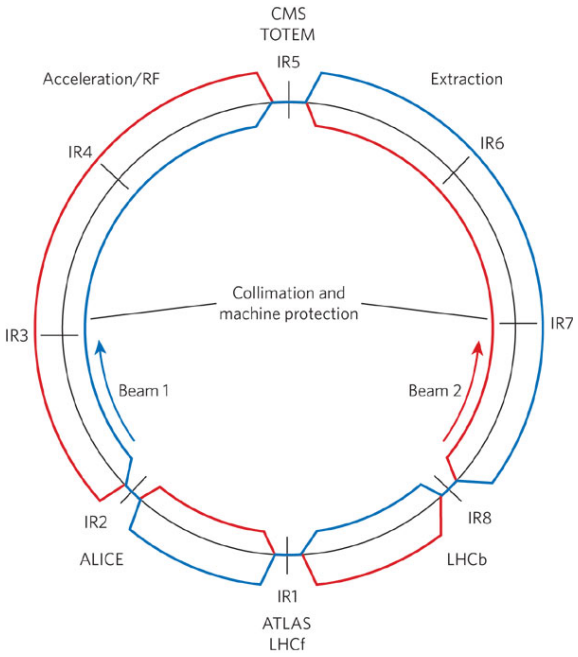

Figure 2: Layout of the HL-LHC [3]

The FCC-hh (Fig. 1) is a 100 km proton-proton collider project in the Geneva area that planes to achieve a centre-of-mass energy of 100 TeV. This accelerator is composed of two high-luminosity interaction points (IPA and IPG) and of two other ones with lower luminosity (IPH and IPF).

The HL-LHC (Fig. 2) is an upgrade of the LHC that planes to increase its luminosity by a factor 10 beyond the original design value. Four interaction points constitute this machine too : Alice and LHCb (located at IP2 and IP8), Atlas and CMS (main ones located at IP1 and IP5).

Note that for both accelerators, only the two main experiments (IPA & IPG and IP1 & IP5 respectively) will be studied.

2 Theoretical approach

2.1 Beam-beam interaction

The nature of the force previously discussed is either focusing or defocusing, depending on the charge of one particle with respect to the other. In our case, only proton-proton collisions will be considered so that the particles have the same charge and the force is defocusing.

In order to study the effects of the electromagnetic field induced by a bunch, one can make the acceptable assumption that the distribution function of the particles in the latter is close to Gaussian. In the two-dimensional case, the charge density Gaussian distribution is :

$$\rho_u(u) = \frac{1}{\sigma_u\sqrt{2\pi}} \exp\left(-\frac{u^2}{2{\sigma_u}^2}\right) \qquad \text{where } u = x, y \tag{2}$$

such that σ_x and σ_y represent the r.m.s. size of the bunch.

The following discussion is valid for round beams, which means $\sigma_x = \sigma_y = \sigma$. Note that this assumption is not always acceptable : typically in the case of e^+-e^- ring, synchrotron radiation effects on the beam shape are not negligible and the beam should then be considered as being elliptical. The round beam approximation is however valid in our case since the synchrotron radiation is weak in the machine studied and therefore does not affect the particle distribution.

The force acting on a particle of charge q and due to an electromagnetic field is given by the Lorentz force :

$$\vec{F} = q(\vec{E} + \vec{v} \wedge \vec{B}) \tag{3}$$

where E and B corresponds to the electric and magnetic field respectively and v to the velocity of the particle. The latter can be rewritten in cylindrical coordinates and by taking the radial component, we obtain :

$$F_r = q(E_r + vB_\theta) \tag{4}$$

Using the expression of the two-dimensional potential from a Gaussian beam with a Gaussian charge distribution (Eq. 2), one can express the radial force for a particle travelling in the opposite direction [1] :

$$F_r(r) = -\frac{nq^2(1+\beta^2)}{2\pi\epsilon_0}\frac{1}{r}\left[1 - \exp\left(-\frac{r^2}{2\sigma^2}\right)\right] \tag{5}$$

where n is the line density of particles in the beam, ϵ_0 the vacuum permittivity and β corresponds to the normalized speed of the particles. A sketch of the radial force as a function of the amplitude is given in Fig. 3.

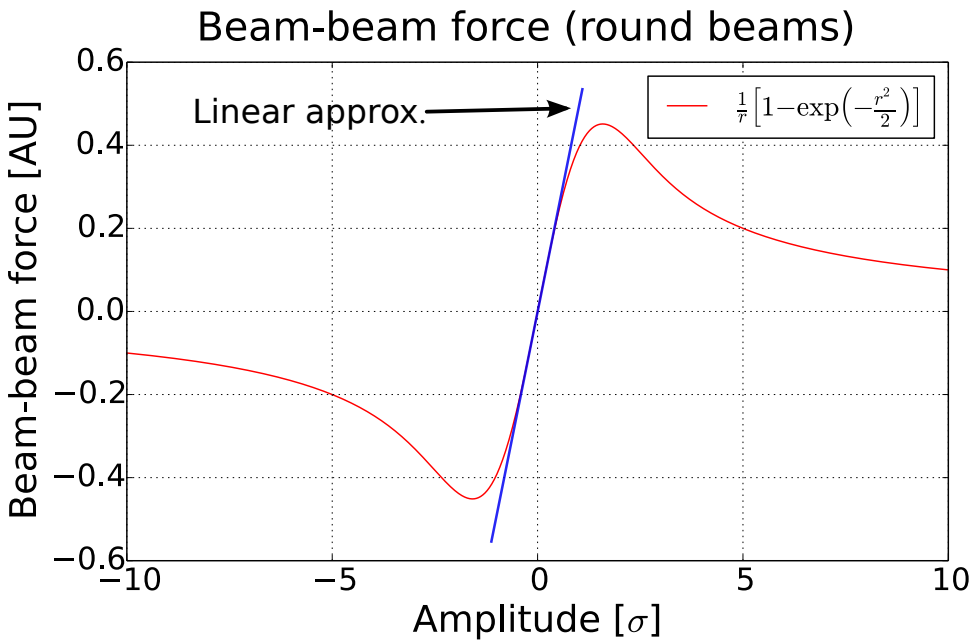

Figure 3: Beam-beam force for round beams with the linear approximation for small amplitudes

As one can see for small amplitudes (i.e. below $\approx 1\sigma$), the force is approximately linear, meaning that the force from the round Gaussian bunch near its axis is linear :

$$F_r \cong -\frac{Nq^2(1+\beta^2)}{4\pi\epsilon_0\sigma^2} r \tag{6}$$

where N is now the total number of particles.

Consequently, the particle travelling sees the beam coming from the opposite direction as a defocusing quadrupole when they are close enough. Indeed, one can recall that the magnetic field of such element is proportional to the distance from the axis ; the defocusing property comes from the sign of the force. The particle experiences then a kick from the opposite beam leading to the change of the beam dynamics. In particular, the quadrupole component changes the optics. To understand the dynamics of particle oscillating with a large amplitude, the higher order components need to be taken into account.

In order to derive the expression of the kick received, one should start from the expression of the force (Eq. 5) and multiply it by the longitudinal distribution depending on position and time. The expression obtained should then be integrated over the collision (Newton's law) to get the radial deflection. We finally get [1] :

$$\Delta r' = -\frac{2Nr_0}{\gamma} \cdot \frac{1}{r} \cdot \left[1 - \exp\left(-\frac{r^2}{2\sigma^2}\right)\right] \tag{7}$$

where r_0 stands for the classical particle radius and γ corresponds to the Lorentz factor. For small amplitudes r (linear effects), the corresponding kick can be derived by taking the limit $r \to 0$ of the previous equation :

$$\Delta r'|_{r\to 0} = -\frac{Nr_0}{\gamma\sigma^2}r = -\frac{1}{f}\cdot r \tag{8}$$

The factor $1/f$ is actually the slope of the force at $r = 0$. Let us now introduce a quantity ξ known as the linear beam-beam parameter that can be interpreted as the strength of the beam-beam interaction in the linear region :

$$\xi = \frac{Nr_0\beta^*}{4\pi\gamma\sigma^2} = \frac{\beta^*}{4\pi f} \tag{9}$$

where β^* is the value of the β-function at the interaction point. One of the interest of the variable ξ is that for a tune far enough from linear resonances (half-integer and integer tune) and for small amplitudes, the tune shift induced by the interaction of the beams is equal to the beam-beam parameter.

2.2 Theoretical formulas

In order to check the code and the results given by MAD-X, one can compare the variation of some specific quantities due to one beam-beam interaction to some analytical formulas. The latters can be derived by making the assumption that a beam-beam interaction is equivalent to a defocusing quadrupole introduced in the lattice. This method will permit us to see the linear effects of a head-on collision on the optics in the accelerator. The complete development of the following formulas with the calculations can be found in [1], the idea of the derivations will however be exposed briefly. Finally, note that the round beam assumption is kept for the development of these formulas.

If one is placed at the interaction point, the change of the value of the β-function can be calculated. More specifically, the relation between the β-functions at an interaction point β^*/β_0^* can be deduced from the one turn maps before and after the beam-beam interaction (M_0 and M) and the transformation matrix of a defocusing quadrupole Q_D. One should make an additional assumption too : the β-functions (on both planes) are minimum at the interaction points before and after perturbation ($\alpha_0 = \alpha = 0$) :

$$\underbrace{\begin{pmatrix} \cos(\mu) & \beta\sin(\mu) \\ -\frac{1}{\beta}\sin(\mu) & \cos(\mu) \end{pmatrix}}_{M} = \underbrace{\begin{pmatrix} 1 & 0 \\ \frac{1}{2f} & 1 \end{pmatrix}}_{Q_D} \cdot \underbrace{\begin{pmatrix} \cos(\mu_0) & \beta_0\sin(\mu_0) \\ -\frac{1}{\beta_0}\sin(\mu_0) & \cos(\mu_0) \end{pmatrix}}_{M_0} \cdot \underbrace{\begin{pmatrix} 1 & 0 \\ \frac{1}{2f} & 1 \end{pmatrix}}_{Q_D} \tag{10}$$

where the 0 index refers to the unperturbed Twiss parameters, f to the focal length of the quadrupole modelling the beam-beam interaction and μ to the phase advance whose definition is

$$\mu_{x,y} = 2\pi Q_{x,y} = \oint \frac{1}{\beta_{x,y}(s)}\,\mathrm{d}s \tag{11}$$

such that the integral is performed all around the machine, $Q_{x,y}$ corresponds to the tune

in a specific plane (horizontal or vertical) and s is the position in the accelerator relatively to the reference orbit.

Making the above calculations and using some trigonometric relations, one can deduce the relation of the β-beating at the interaction point :

$$\frac{\beta^*}{\beta_0^*} = \frac{1}{\sqrt{1 - 4\pi\xi\cot(\mu_0) - 4\pi^2\xi^2}} \tag{12}$$

The relative variation of the β-function due to a quadrupole field error at a position s can also be derived theoretically. The procedure is similar as the previous calculation by evaluating the perturbed one turn map. One should then use the transport matrices in order to calculate the quadrupole error on the β-function at any location in the ring.

$$\frac{\Delta\beta(s)}{\beta_0(s)} = \frac{2\pi\xi}{\sin(2\pi Q_0)}\cos(2|\mu_0(s) - \mu_0(s_0)| - 2\pi Q_0) \tag{13}$$

It is also possible to derive analytically the change of the β-function coming from N small quadrupole errors at positions s_i $(i = 1, ..., N)$ considering small perturbations, therefore the variations add up linearly [4] :

$$\frac{\Delta\beta(s)}{\beta_0(s)} = \frac{2\pi\xi}{\sin(2\pi Q_0)}\sum_{i=1}^{N}\cos\left(2|\mu_0(s) - \mu_0(s_i)| - 2\pi Q_0\right) \tag{14}$$

In case of beam losses, the latters will happen where the aperture is the smallest and this might likely occurs where the maximum of the β-beating is. Therefore one should minimize the maximum of the β-beating whose expression can be derived from Eq. 13 :

$$\max\left(\frac{\Delta\beta}{\beta_0}\right) = \frac{2\pi\xi}{\sin(2\pi Q_0)} \tag{15}$$

Beam-beam interactions not only change the β-function but also the tune of the machine. Indeed, the additional element will affect the β-function around the accelerator and consequently the tune given its definition (Eq. 11). One can estimate this change using the same idea as for the derivation of Eq. 12. The one turn map gives then easily access to the total tune in the storage ring. Finally, for small tune shifts $\Delta Q = Q - Q_0$, one can write :

$$\cos(2\pi Q) = \cos(2\pi Q_0) + 2\pi\xi\sin(2\pi Q_0) \tag{16}$$

3 MAD-X program

MAD-X is a general purpose beam optics and lattice program for machine design and simulation.

The latter describes the machine by a set of elements each represented by a first or second order transfer matrix, which all together gives the one turn matrix from which one finds the fixed points, i.e. the orbit, and the eigenmodes, i.e. the periodic solutions, that can be expressed as optics (or Twiss) functions ([5] & [6]).

The main steps of resolving are the following :

- A general vector differential equation is derived describing the trajectory of a charged particle in an arbitrary static magnetic field with "midplane symmetry".
- A Taylor's series solution about the central trajectory is then assumed; this is substituted into the general differential equation and terms to second-order in the initial conditions are retained.
- The first-order coefficients of the Taylor's expansion (for mono-energetic rays) satisfy homogeneous second-order differential equations characteristic of simple harmonic oscillator theory and the first-order dispersion and the second-order coefficients of the Taylor's series satisfy second-order differential equations having "driving terms".
- The first-order dispersion term and the second-order coefficients are then evaluated via a Green's function integral containing the driving function of the particular coefficient being evaluated and the characteristic solutions of the homogeneous equations.

3.1 Matching algorithms

Since the optics is a very non-linear function of the strength of all elements in the machine, one needs to use a matching algorithm to find the variation of strength needed to obtain a controlled variation of a given optics parameter. In this algorithm, one should specify the global constraints (e.g. the horizontal tune Q_x) and the local constraints (e.g. the value of a twiss parameters at a specific location like β_y^*) we want.

From this point, the program computes the penalty function, defined as the normalized measure of the violation of the constraints and aims to minimise it by varying a given set of parameters, e.g. the strength of some quadrupoles, so that the machine verifies the wanted constraints.

Two algorithms have mainly been used through the simulations to minimise the penalty function : Levenberg-Marquardt and Newton's algorithm.

The Newton's algorithm (called *JACOBIAN* in MAD-X) is able to solve a generalized matching problem with an arbitrary number of variables and constraints [7]. The algorithm is actually based on the Newton-Raphson method. As an example, let us take a matching problem defined as

$$\vec{c} = \mathbf{f}(\vec{v}) \tag{17}$$

where $\vec{c}$ corresponds to the vector of c constraints, $\vec{v}$ to the vector of v variables and $\mathbf{f}$ is the vector field representing the machine observables. If $\vec{c}_0 = \mathbf{f}(\vec{v}_0)$ is a solution for $\vec{c}_0$ close to $\vec{c}$, one can write

$$\vec{c} = \vec{c}_0 + \mathbf{J}(\vec{v}_0)\delta\vec{v} + O\left(|\delta\vec{v}|^2\right) \tag{18}$$

where $\mathbf{J} = \frac{D\mathbf{f}}{D\vec{v}}$ is the Jacobian of the transformation $\mathbf{f}$ and $\delta\vec{v}$ the vector which points to the solution. The solution is found iteratively using the following relations :

$$\vec{v} = \vec{v}_0 + \alpha_n\delta\vec{v} \qquad\qquad \delta\vec{v} = \mathbf{J}^{-1}(\vec{c} - \vec{c}_0) \tag{19}$$

where α_n is the succession 2^{-n} and n is chosen such that the penalty function $|\vec{c} - \vec{c}_0|$ is smaller than the previous step.

If $\mathbf{J}$ is a square matrix ($c = v$) the system can be inverted exactly. In the case where the matrix is rectangular ($v > c$ or $v < c$), the system is inverted by a QR or LQ decomposition yielding the minimization of $|\vec{c} - \vec{c}_0|$ or $|\delta\vec{v}|$ respectively. Note that this method requires to be sufficiently close to the solution.

The Levenberg-Marquardt algorithm in MAD-X (called *LMDIF*) is an iterative technique that is generally the fastest minimisation method but limited to problems where the number of variables is not greater than the number of constraints. Also the constraints have to be differentiable in order to avoid numerical instabilities.

This algorithm interpolates between the Gauss-Newton algorithm and the gradient descent. This mixing makes the algorithm more robust than the Gauss-Newton algorithm, in the sense that it will in many cases find a solution even if it starts far from the minimum. When the current solution is close to the correct solution, it becomes a Gauss-Newton method. Let us take the same situation as for the Newton's algorithm.

The Levenberg-Marquardt method solves equations called the augmented normal equations [8] :

$$\mathbf{N}\delta\vec{v} = \mathbf{J}^T(\vec{c}_0 - \vec{c}) \tag{20}$$

where the off-diagonal elements of $\mathbf{N}$ are equal to the elements of $\mathbf{J}^T\mathbf{J}$ and the diagonal elements are given by $\mathbf{N}_{ii} = \mu + \left[\mathbf{J}^T\mathbf{J}\right]_{ii}$ for $\mu > 0$ called the damping term. If the updated parameter vector $\vec{v} + \delta\vec{v}$ with $\delta\vec{v}$ computed from Eq. 20 leads to a reduction in the error of $(\vec{c}_0 - \vec{c})$, the update is accepted and the process repeats with a decreased damping term. Otherwise, the damping term is increased, Eq. 20 are solved again and the process iterates until a value of $\delta\vec{v}$ that decreases the error is found. The process of repeatedly solving Eq. 20 for different values of the damping term until an acceptable update to the parameter vector is found corresponds to one iteration of the algorithm. The damping term is adjusted at each iteration to assure a reduction in the error $(\vec{c}_0 - \vec{c})$.

4 Simulations and discussion

Several numerical evaluations of optics functions have been performed using different configurations on the two different accelerators : one and two beam-beam interactions have been respectively created in the main interaction points of the FCC-hh and of the HL-LHC.

4.1 Collimation system

The imbalance between the arcs IP1-IP5 and IP5-IP1 or IPA-IPG and IPG-IPA has a different impact on the collimation insertions. The HL-LHC is composed of two collimation insertions at IR3 and IR7 (Fig. 2). Therefore, the beating in both arcs needs to be minimized. In the FCC-hh, several options remain possible, having an unbalance between the two arcs could remain a viable option. In other words, one could have in the FCC-hh only one collimation insertion on the "good" side, i.e. in the arc where the beating is the least.

Note that since the cleaning concerns mainly the particles in the tail, i.e. the ones that oscillate with a large amplitude, and that only the linear effects with head-on collisions are discussed, the analysis presented in the following pages does not apply. The non-linear dynamics of the particles in the tail, as well as their interaction with the collimation system will be studied later using a different approach.

4.2 Benchmark against the code

This section is dedicated to benchmark the numerical evaluations run on MAD-X against the theoretical formulas presented in Sec. 2.2 for the FCC-hh and the HL-LHC. More precisely, the beam-beam interaction occurs at IPA for the FCC-hh and at IP1 for the HL-LHC.

The first set of simulations was done by performing a scan on the beam-beam parameter ξ. The strength of the beam-beam interaction is varied using the number of particles per bunch, while keeping a constant normalised emittance. The several quantities were then deduced from each set of simulations : the β-beating at the IP (Eq. 12), the maximum of the β-beating (Eq. 15) and the tune shift ΔQ (Eq. 16).

As we can see on Fig. 4, simulations concord with the formula given by Eq. 12. Indeed, the relative error between the values of the β-beat and the formula is in the order of 10^{-7}. The same simulations have been run with the HL-LHC and provided similar results : the relative error in that case was around 10^{-10}. This shows that MAD-X implements correctly the physics model of the interaction.

Concerning the tune shift (Fig. 5) for the FCC, the results provided by the simulations and the theoretical formula (Eq. 16) seem to correspond in both planes. Indeed, one can calculate that the relative error was always below 10^{-5}. Note that the same set of simulations has been performed with the HL-LHC and that the conclusions are identical

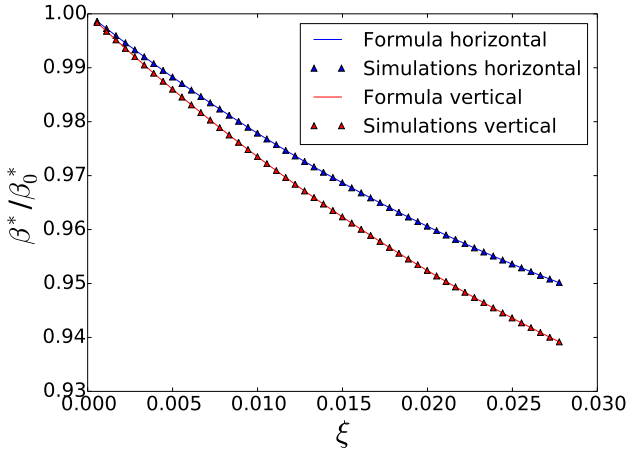

Figure 4: β-beating at IPA due to beam-beam interaction at IPA

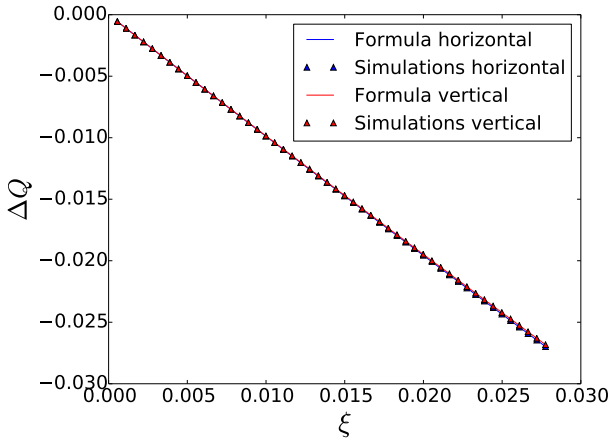

Figure 5: Tune shift due to beam-beam interaction at IPA

to the ones of the FCC. This means that the beam-beam interaction is in these cases well approximated by the presence of a defocusing lens at the same position.

Then, the maximum of the β-beating on the whole machine has been found for each beam-beam prameter ξ (Fig. 6) and compared to the related theoretical formula (Eq. 15). As one can see, the agreement is not as good as in the previous cases. The graph given in Fig. 7 shows the relative error between the simulations and the expected values from the theoretical formula. We can observe that the error is acceptable for a small intensity and increases almost linearly with the beam-beam parameter ξ. This indicates that the derived formula is acceptable in the approximation of a small beam-beam parameter. Note that the same simulations have been run with the HL-LHC and provided equivalent results.

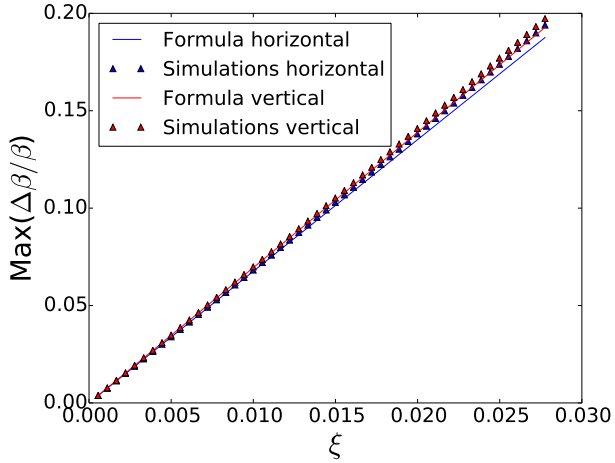

Figure 6: Maximum β-beating due to beam-beam interaction at IPA

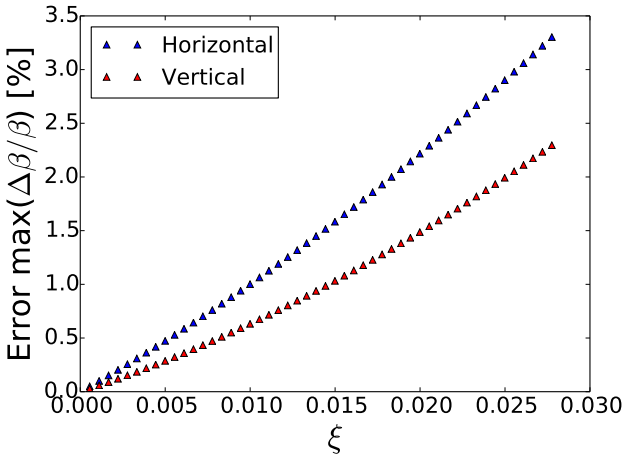

Figure 7: Relative error of the maximum of the beating with respect to Eq. 15

The second set of simulations consists in a scan on the unperturbed horizontal tune $Q_{x,0}$, i.e. the tune of the machine before the beam-beam interaction. In practice, the initial horizontal tune $Q_{x,0}$ was modified repeatedly by performing a matching sequence

that varied the strength of the two families (focusing and defocusing) of quadrupoles in the arc cells. On top of that, for each matching, the following constraints were set : the β-function for both planes should remain the same before and after the matching sequence at the interaction point were the beam-beam interaction was put and the α parameter was forced to be zero at the same place to insure that the IP is located at the minimum of the β-function.

Since the tune Q appears in sinus or cosine functions only, this implies that the integer part of the latter does not change the optics of the beam. This is why the scan of the unperturbed horizontal tune $Q_{x,0}$ will start from 108.0 to 108.5 for the FCC-hh and from 62.0 to 62.5 for the HL-LHC. However, as one will be able to notice, the scan performed on $Q_{x,0}$ doesn't cover all the required range. This is actually due to the fact that as soon as $Q_{x,0}$ is near an integer or half-integer, one is close to resonances of the machine which drives the optics function towards infinity just by adding the beam-beam interaction.

As we can see on Fig. 8, the simulations performed including a beam-beam interaction at IPA are consistent with the previously deduced theoretical formula of the optics distortion due to the introduction of a beam-beam interaction (Eq. 12). The relative error of the simulations compared to the formula is always below 10^{-8} which means that the beam-beam interaction is well modelled by the presence of a defocusing quadrupole at the interaction location. Similar conclusions can be drawn for the HL-LHC optics.

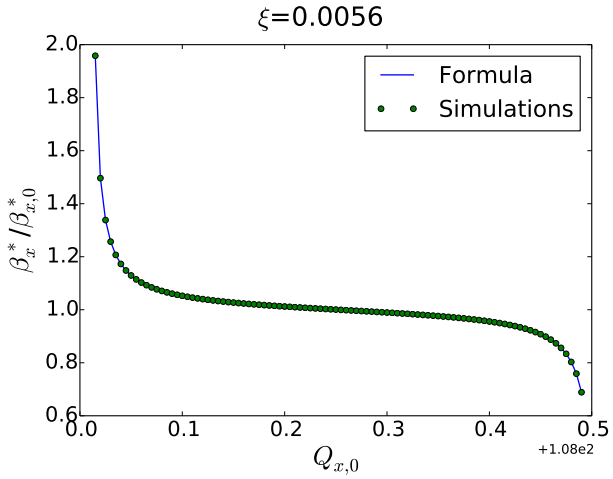

Figure 8: Horizontal β-beat at IPA due to beam-beam interaction at IPA

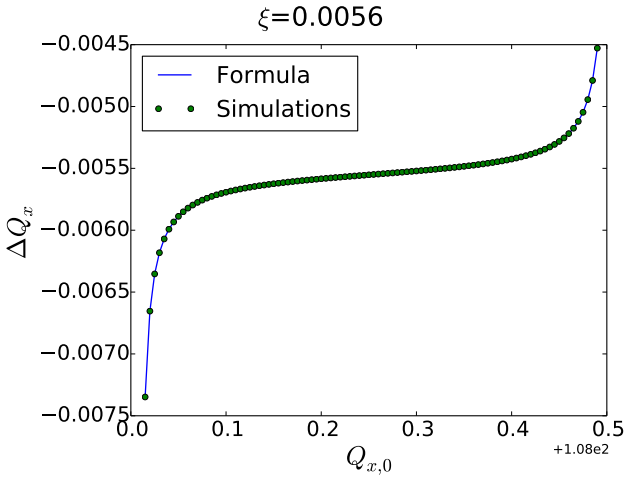

Figure 9: Horizontal tune shift due to beam-beam interaction at IPA

Concerning the horizontal tune shift induced by a beam-beam interaction at IPA shown in Fig. 9, the simulations and the formula (Eq. 16) also agree. Indeed, one can calculate that the relative error is about 10^{-5} for the FCC, which indicates that the beam-beam interaction is one more time well simulated by a defocusing lens. Equivalent results have been found for the HL-LHC where the error was about 10^{-6}. The value of the tune shift ΔQ_x is equal to the beam-beam parameter ξ when one is far from resonances points as expected too.

As we can see on Fig. 10 and 11, the comparison between the simulations and the formula (Eq. 15) doesn't provide as good results as before concerning the maximum of the β-beating in the machine. Indeed, in this case the relative error reaches 60% when we are close to the integer or half-integer and gets close to zero for a tune $Q_{x,0} \approx 108.335$. In this case too, similar results have been found for the HL-LHC with a relative error of the same order. This error gets close to zero for an unperturbed tune around $Q_{x,0} = 62.335$. However, a precise explanation for the disagreement close to resonance could not be found.

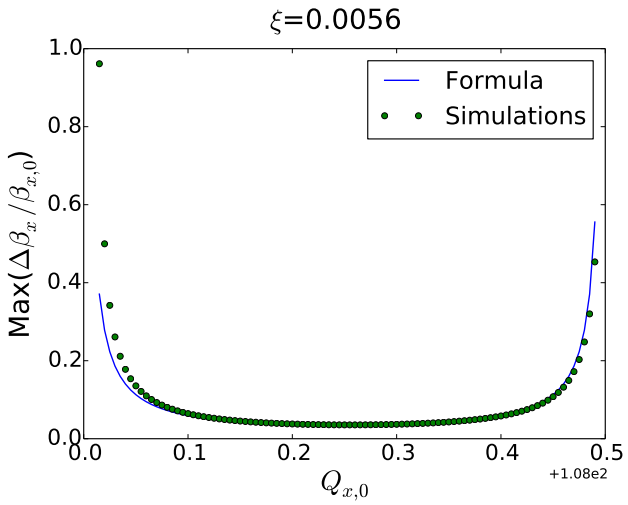

Figure 10: Maximum of the horizontal β-beating due to beam-beam interaction at IPA

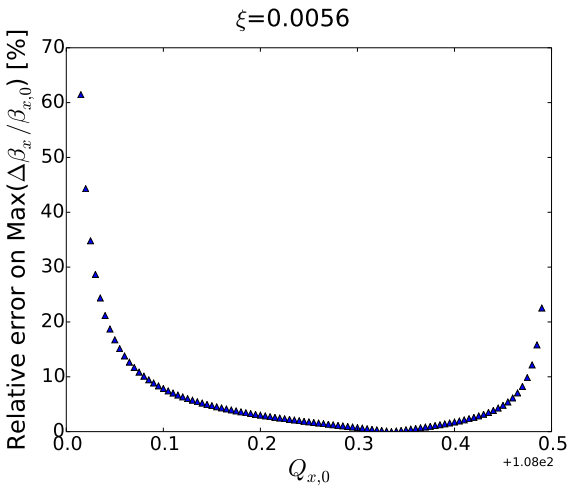

Figure 11: Relative error with respect to Eq. 15 of the maximum of the horizontal β-beating

Finally, similar simulations with a beam-beam interaction at IPG (respectively IP5) always lead to similar results, resulting from the symmetry between both main interaction points for both accelerators.

4.3 β-beating with one beam-beam interaction

First of all, let us take a look at the initial unperturbed β-function shown in Fig. 12. Note that the latter is similar for both accelerators ; the differences come from the scales.

The head-on beam-beam interaction at IPA in the FCC-hh induces then a change in this β-function represented in Fig. 13. One can see that the β-beating affects approximately the same way both planes, in other words, the value of the maximum of the beating is roughly the same. One can also mention that it has been observed that the beating is proportional to the beam-beam parameter ξ as expected thanks to Eq. 13.

Taking a closer look at both main IP's provides indications about the layout and the shape of the β-function in the interaction regions (Fig. 14 and 15). Indeed, as one can see, the beating modulates in three different ways. Firstly, the latter is periodic at the end of each IP. Secondly, the beating remains approximately constant close to both sides of the IP. Finally, at the interaction point, one can observe that this latter is characterized by a

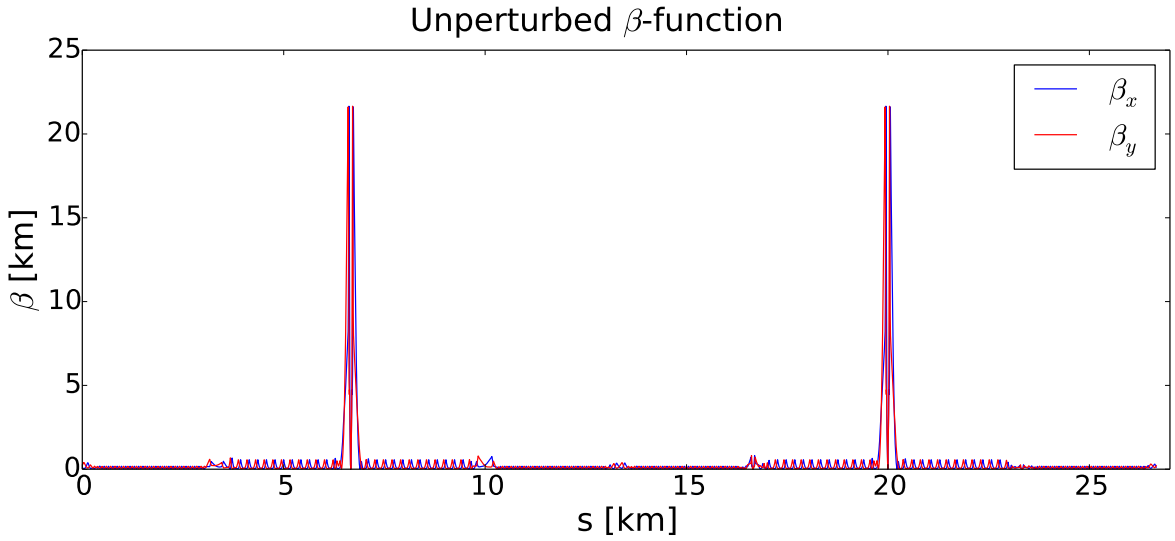

Figure 12: β-function through the HL-LHC for both planes

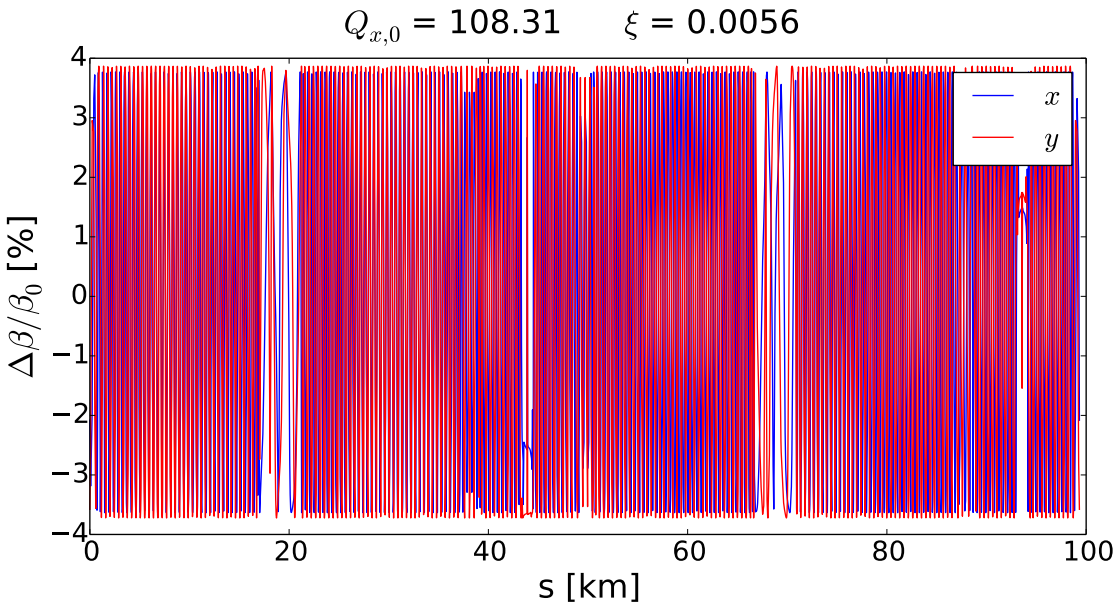

Figure 13: β-beating in the entire FCC for both planes

big variation of the beating which consists in a peak upwards or downwards depending on which IP we examine.

For the first part (the end of each IP), it can be explained by the periodicity of the lattice constituted of FODO cells (Fig. 12). Concerning the two last parts, one should use the relation between the β-function and the phase advance (Eq. 11) to study the impact on the beating. Indeed, the beating depends on the phase advance with respect to the beam-beam interaction (Eq. 13). Since the β-function is very small at the interaction point, the phase advance will strongly change with respect to s, so that the beating will vary a lot at this point. When one is on the side of the IP, the β-function is very large such that the phase advance will dimly change with s and therefore the variation of the beating is small.

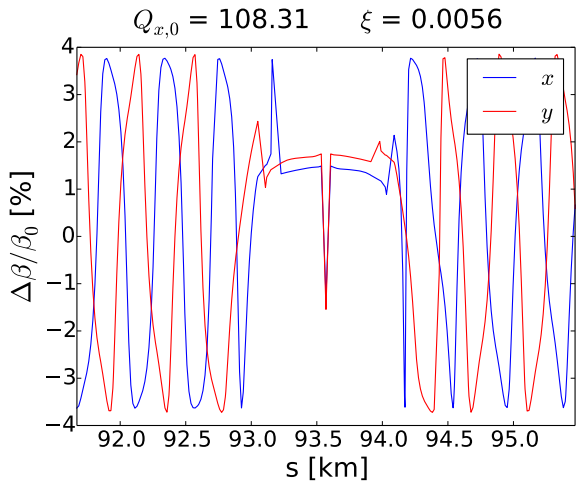

Figure 14: β-beating at IPA due to beam-beam interaction at IPA

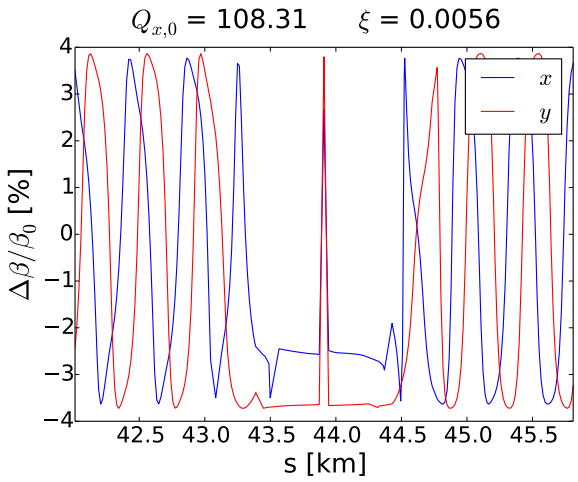

Figure 15: β-beating at IPG due to beam-beam interaction at IPA

It is also interesting to study the influence of the unperturbed horizontal tune $Q_{x,0}$ on the beating always induced by the beam-beam interaction. To analyse the effect of this initial parameter, the latter has been changed (using the arc quadrupoles) and brought closer to an half-integer (Fig. 16 and 17).

For these graphs, only the horizontal component is represented because no changes in the vertical beating has been observed as the initial horizontal tune $Q_{x,0}$ was modified : the matching process of the tune on the horizontal plane didn't affect the β-beating on the vertical plane.

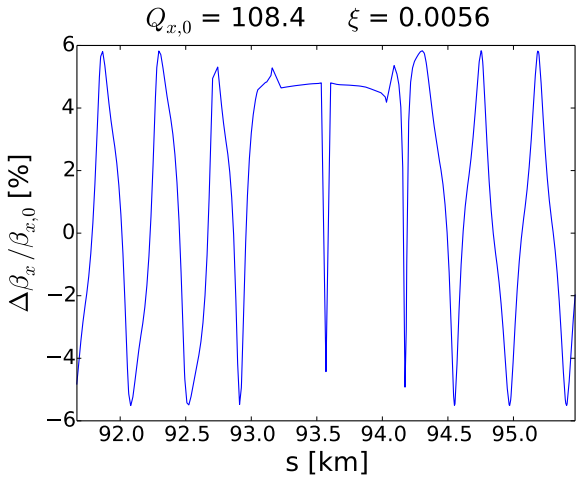

Figure 16: β-beating at IPA due to beam-beam interaction at IPA

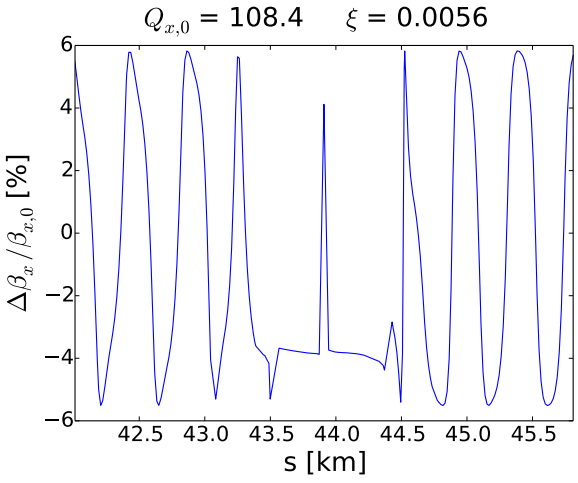

Figure 17: β-beating at IPG due to beam-beam interaction at IPA

One can notice on Fig. 16 and 17 that the layout can still be figured out as previously using the same reasoning. The important change is that once we move sufficiently away from the original tune ($Q_{original}$ = 108.31), the horizontal component of the β-beating increases, however, the shape of the latter remains roughly the same for both interaction points whatever the initial tune $Q_{x,0}$ is. This rise of the beating can be easily explained

by looking at the Eq. 13 : the further we are from $Q_{x,0} = 108.25$, the closer we are to an integer or half-integer value of the tune which makes the factor sinus smaller and consequently increases the β-beating.

Note that the previous results given were always equivalent to the ones provided by the simulations where the beam-beam interaction was placed at IPG, meaning that Fig. 14 and 16 would correspond to the β-beat at IPG and Fig. 15 and 17 to the one at IPA. This phenomenon is actually due to the fact that the current FCC-hh lattice is symmetric with respect to the two main interaction points IPA and IPG.

Concerning the HL-LHC, one can make the same analysis by placing one beam-beam interaction at IP1 and observe the effects of the latter on the Twiss parameters. The β-beating through the entire machine is represented in Fig. 18.

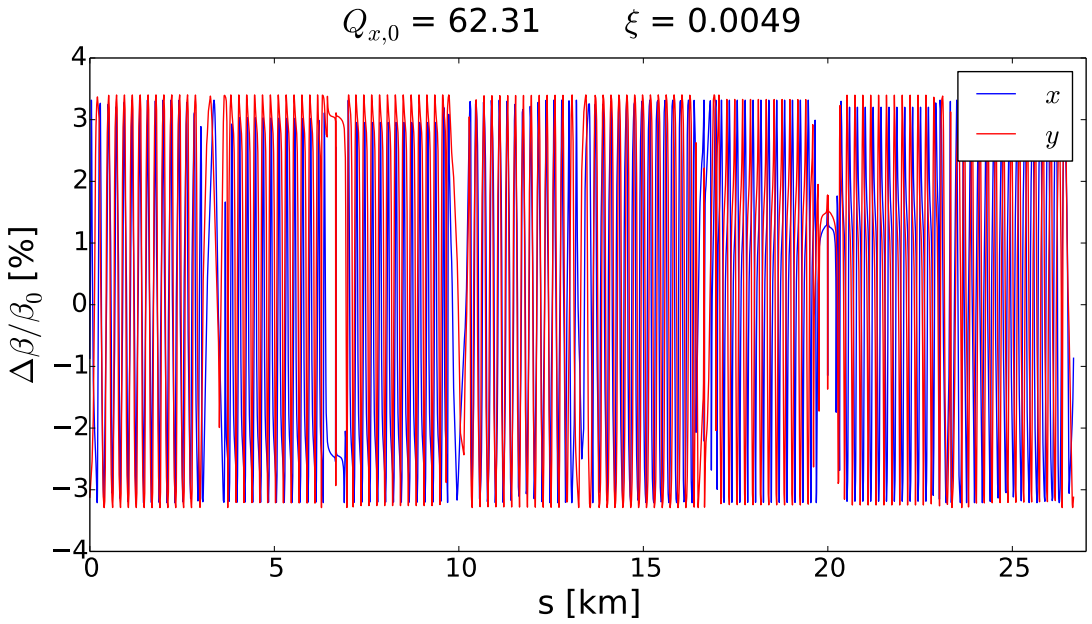

Figure 18: β-beating in the HL-LHC in both planes

The same statement can be done for the β-beating (Fig. 18) in the HL-LHC as in the FCC-hh : both planes are affected approximately the same way. The proportionality with respect to the beam-beam parameter ξ is verified with this lattice as expected too.

The beating at both IP's is given in Fig. 19 and 20 and the same analysis with the three parts can be done as previously. The shape of the beating in the HL-LHC differs however slightly from the one with the FCC-hh ; this comes from the fact that the phase advance is different with respect to the FCC-hh and that the design of the insertion is a little different.

Note that the previous results given for the β-beat are similar to the ones provided by the simulations where the beam-beam interaction was placed at IP5 in the HL-LHC, which means that Fig. 19 looks like the β-beat at IP5 and Fig. 20 like the one at IP1. The differences come from the phase advance of the beating of one plane with respect to another and the shape which is slightly different because the lattice is not fully symmetric.

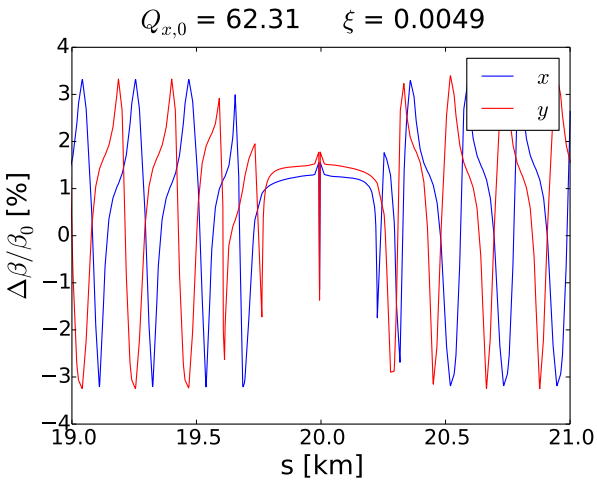

Figure 19: β-beating at IP1 due to beam-beam interaction at IP1

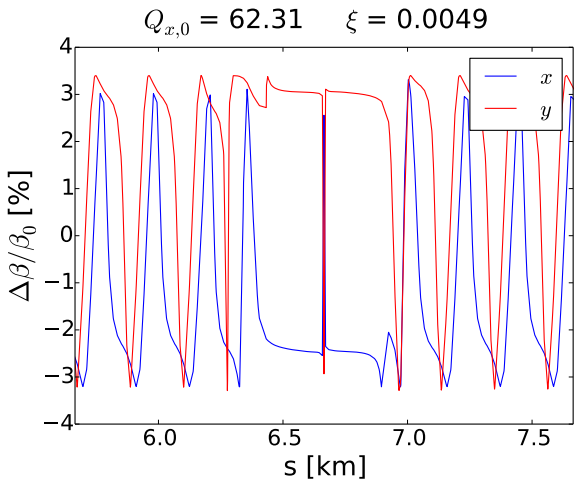

Figure 20: β-beating at IP5 due to beam-beam interaction at IP1

Finally, the same computations concerning the effect of the unperturbed tune $Q_{x,0}$ have been made for the HL-LHC and equivalent conclusions as for the FCC-hh can be drawn (Fig. 45 and 46 in the appendix).

4.4 Two beam-beam interactions

Let us study now the beam dynamics when two beam-beam interactions are present simultaneously at IPA and IPG respectively for the FCC-hh. The same quantities will be studied and compared to the case with one beam-beam insertion.

As one could have expected, the two beam-beam interactions perturb the beams dynamics as in the case with only one beam-beam interaction. The effects on the β-functions are clearly visible on Fig. 21.

The significant difference is that the maximum beating relatively to both planes is not in the same order of amplitude any more. As a result, there will be places where the larger beating will correspond to the vertical plane and in return places to the horizontal one.

Another noticeable difference between the situation with one beam-beam interaction and the present one is the change of the amplitude of the beating depending on either we are on the right or the left to an interaction point. Indeed, considering the horizontal plane, one can notice that the amplitude has more than tripled between 44 km and 93.6 km compared to the rest of the machine. This change can be explained thanks to Eq. 14 that indicates that the beating depends on the phase advance relatively to the IP's. An illustration of this dependence is given in Fig. 22 where we clearly see the change of the envelope of the beating. Note that the beating is also proportional to the beam-beam parameter as in the case with one beam-beam interaction.

It is also possible to use Eq. 14 to derive the maximum of the beating knowing the value of the phase advance of the beam between each IP. For this, let us consider Fig. 23 that represents the maximum of the β-beating as a function of the phase advance of the beam.

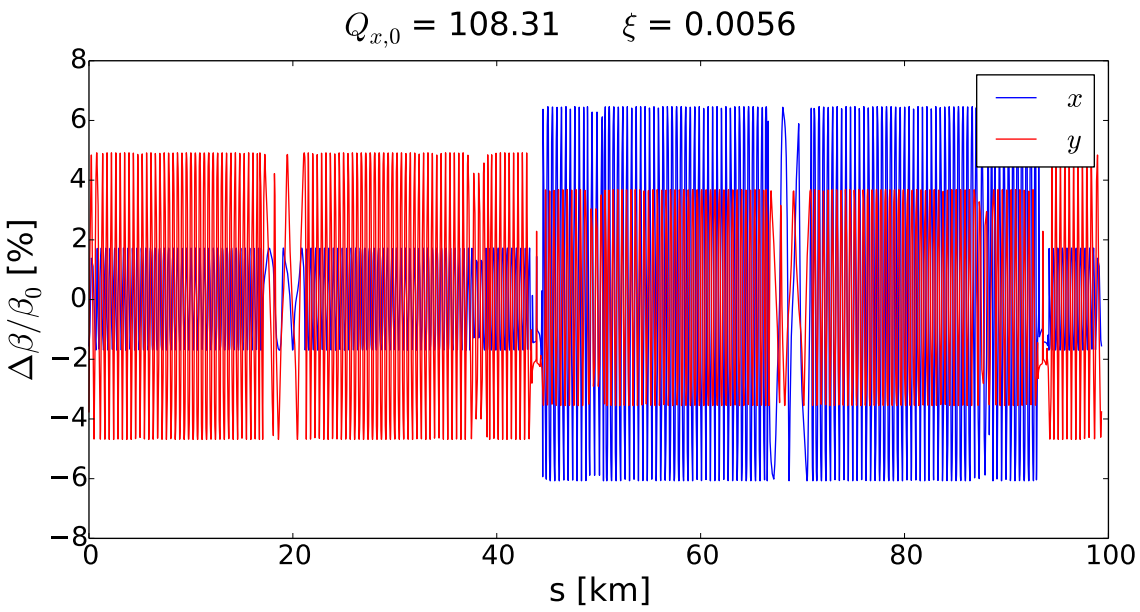

Figure 21: β-beating in the FCC-hh with two beam-beam interactions at IPA & IPG

In the situation where $Q_{x,0} = 108.31$ and $Q_{y,0} = 107.32$, the difference of phase advance of the beam in each plane deduced from the twiss file produced by MAD-X is : $\Delta\mu_{x,0} = 53.93$ and $\Delta\mu_{y,0} = 54.28$ in units of 2π. Computations permits to say that the previous phase advances correspond pretty well to the maximum of the beating relatively to each plane : the error remains below 10^{-2}. This shows that the program predicts acceptably the physics of the two beam-beam interactions. One can also mention that Fig. 23 reveals that by changing the phase advance between each IP, one is capable to distort the maximum of the beating in the machine which is useful.

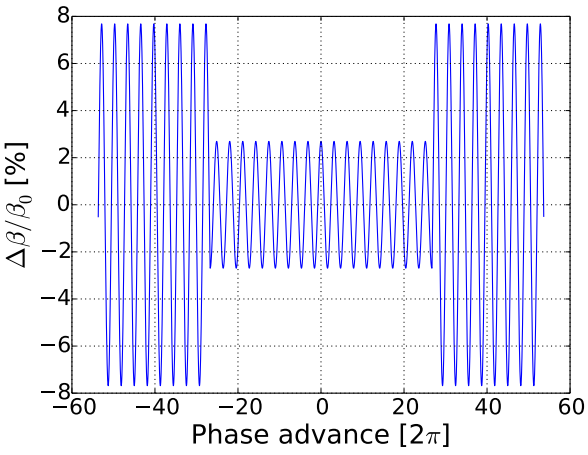

Figure 22: β-beating through the machine with 2 beam-beam interactions derived from Eq. 14

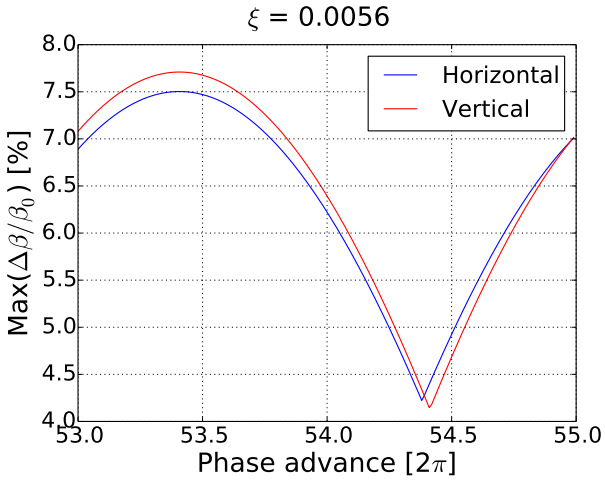

Figure 23: Maximum of the beating as a function of the phase for $Q_{x,0} = 108.31$ and $Q_{y,0} = 107.32$ from Eq. 14

Let's take a closer look at the β-beating at both interaction points IPA & IPG (Fig. 24 and 25 respectively). As one can see, one is still able to recognise the three parts in the interaction region : the periodicity of the beating introduced by the FODO cells, near the IP with a large β-function and a small variation of the beating and finally the IP with a very small β-function that changes strongly the beating.

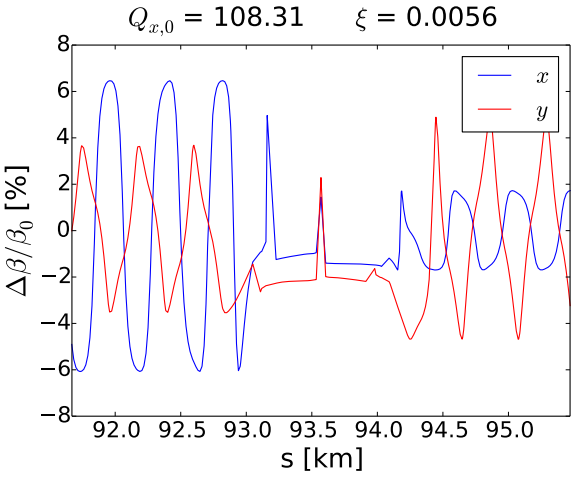

Figure 24: β-beating at IPA due to beam-beam interactions at IPA & IPG

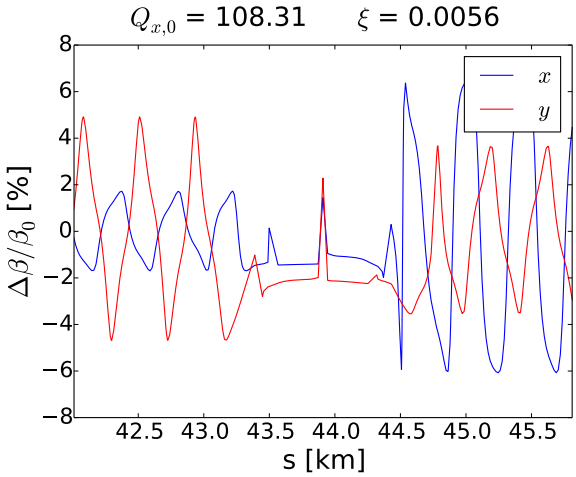

Figure 25: β-beating at IPG due to beam-beam interactions at IPA & IPG

The influence of the initial horizontal tune $Q_{x,0}$ is not as evident as in the case with one beam-beam interaction. Indeed, not only the amplitude of the beating changes with respect to $Q_{x,0}$, but the ratio between the maximum of the beating of each part of an interaction point differs a lot. This makes the analysis of the results much more difficult, this is why only general observations are given.

One can make the observation that the closer we are from $Q_{x,0} = 108.0$, the smaller is the ratio of the maximum between each side of the IP. And in return, the closer we are from $Q_{x,0} = 108.5$, the bigger is this ratio (Fig. 26 and 27). The explanation to this phenomenon can be found in Eq. 14 : the change of the tune will make vary the argument of the cosine functions by subtracting an angle more or less close to $n\pi$ or $2n\pi$ and the beating is proportional to the sum of two cosine functions that have a different argument because each argument of the cosine depends on the phase advance of the IP.

Note that the shape of the β-beating at both IP's is approximately the same whatever the initial horizontal tune $Q_{x,0}$ is. It is very similar to the one shown in Fig. 24 and 25. The differences come mainly from the amplitude of the beating on each side of the interaction point.

As one can see on Fig. 28, the β-beating at the IP's with two beam-beam interactions is very different from the one with only one interaction (Fig. 4) and this is true whatever the plane chosen. Indeed, in the case where we had one beam-beam interaction, the greater was the beam-beam parameter ξ, the smaller was the β-beating at the IP's on both planes. The shape is now the inverse : the β-functions increase in both IP's when the beam-beam parameter increases too. Note that in both cases the change is small : it represents about

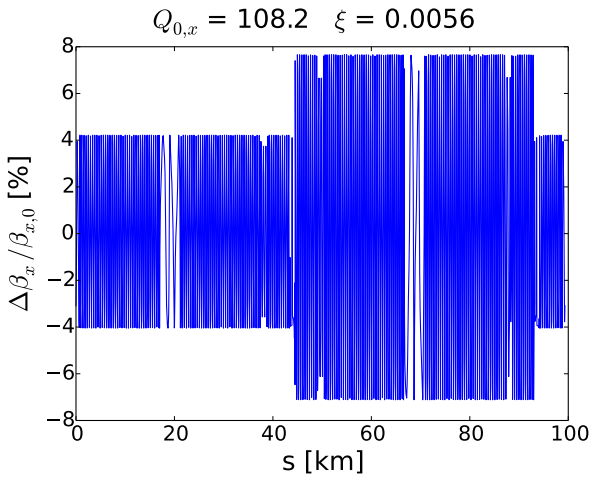

Figure 26: β-beating due to beam-beam interactions at IPA & IPG

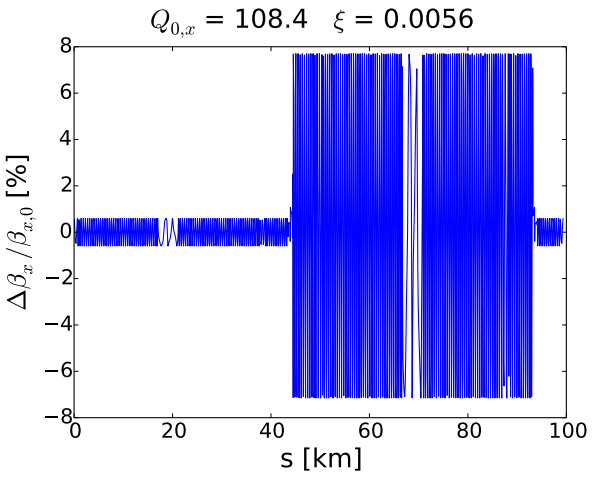

Figure 27: β-beating due to beam-beam interactions at IPA & IPG

10 % when ξ is multiplied by a factor 40. Another point is that both interaction points are very symmetric. In other words, it appears that β^*/β_0^* for each interaction points (IPA & IPG) is very close to each other in both planes : the relative difference is situated around 10^{-8} for the vertical plane and 10^{-10} for the horizontal one.

When a scan is performed on $Q_{x,0}$ for the β-beating at the IP's (Fig. 29), one can see that it is very similar at both interactions points IPA and IPG. Indeed, numerical comparison showed that the relative difference between the two IP's is in the order of 10^{-9}, which shows one more time that the lattice is very symmetric even under the presence of two beam-beam interactions. We can also tell that the curve looks like the one given in Fig. 8 when there only was one beam-beam interaction : the shape and the numerical values are similar.

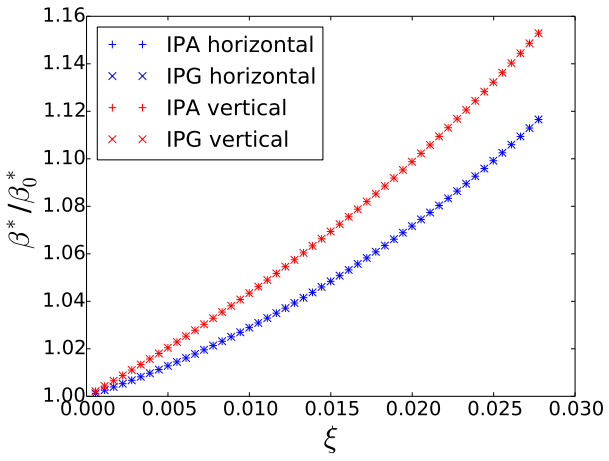

Figure 28: β-beating at the IP's due to beam-beam interactions at IPA & IPG as a function of ξ

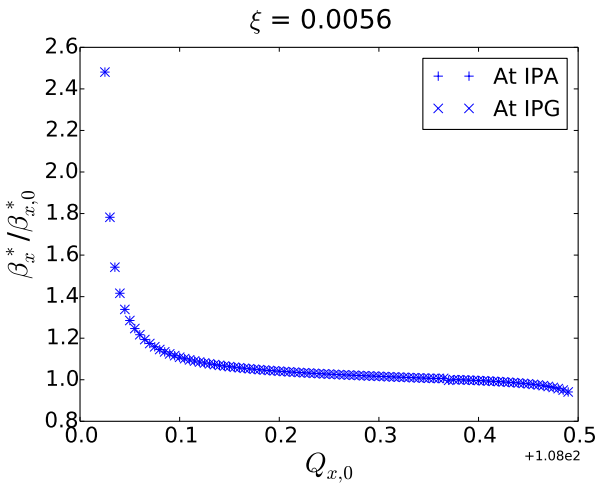

Figure 29: Horizontal β-beating at the IP's due to beam-beam interactions at IPA & IPG as a function of $Q_{x,0}$

Concerning the tune shift due to both beam-beam interactions (Fig. 30), three facts can be highlighted. Firstly, the tune shift is higher in the present case than with only one beam-beam interaction. Secondly, the value of the tune shift is approximately twice bigger than before, which can be impute to the linearity of the effects. Finally, the predominant change of tune occurs in the vertical plane : the situation is inverted with respect to one beam-beam interaction. In the latter case, it was due to the difference in unperturbed tunes and now it should be due to a difference in phase advances. The general behaviour remains however the same for both cases (one and two beam-beam interactions).

The incidence of the initial horizontal tune $Q_{x,0}$ on the horizontal tune shift is given in Fig. 31. The same conclusions as before can be drawn : the curve has the same shape as the one extracted from the simulations with one beam-beam interaction, the scale of the tune shift is however different. Indeed, it is approximately the double of the beam-beam parameter ξ when one is far from from resonances due to linearity of the effect in the small perturbation approximation.

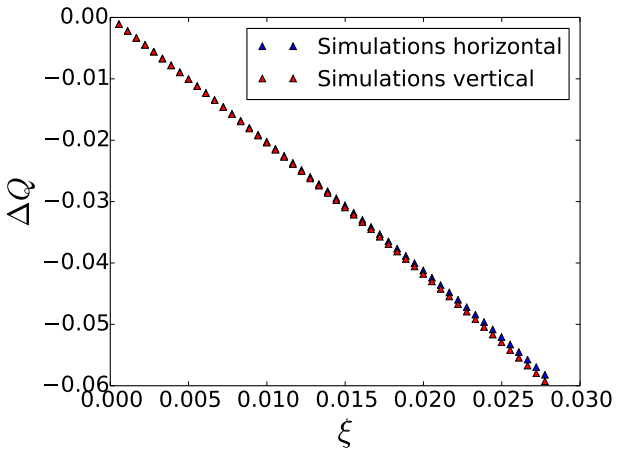

Figure 30: Tune-shift due to beam-beam interactions at IPA & IPG as a function of ξ

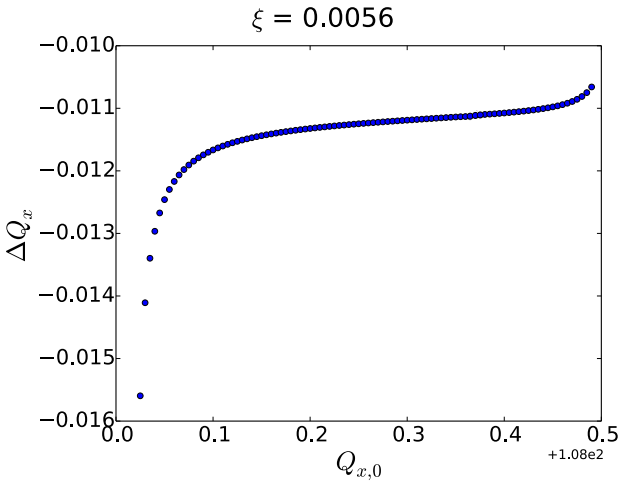

Figure 31: Horizontal tune shift due to beam-beam interactions at IPA & IPG as a function of $Q_{x,0}$

Concerning the maximum of the beating as a function of the beam-beam parameter (Fig. 32), one can notice that it has the same shape as in the case with one beam-beam interaction. The difference between each plane is however more obvious here. The value of the maximum of the beating is a little less than the double of the one with one beam-beam interaction as expected. Indeed, the maximum of a sum of cosine functions is not equal to the sum of the respective maximum of the functions because of the difference of the phase advance between each IP (Eq. 14).

When one does a scan on $Q_{x,0}$ for the same quantity, Fig. 33 is obtained. The shape of the curve is equivalent to the one with one beam-beam interaction, the amplitude of the maximum is however approximately the double in the present case for the same reason as previously.

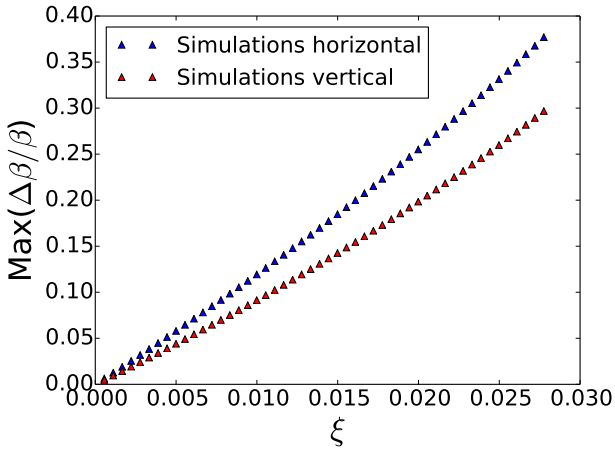

Figure 32: Maximum of the β-beating due to two beam-beam interactions at IPA & IPG as a function of ξ

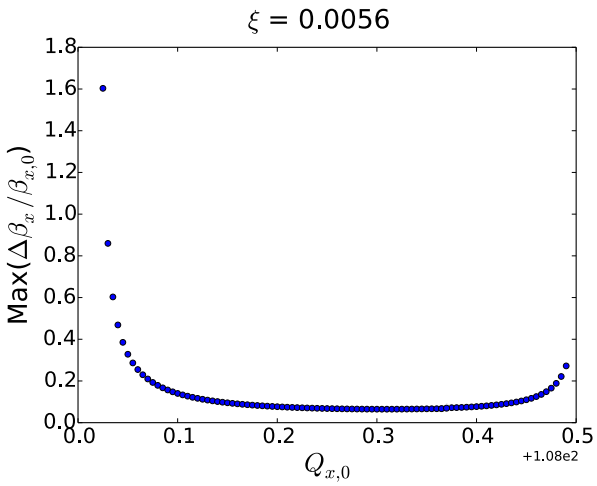

Figure 33: Maximum of horizontal β-beating due to beam-beam interactions at IPA & IPG as a function of $Q_{x,0}$

Let us consider now the HL-LHC. The β-beating induced by two beam-beam interactions at IP1 and IP5 is shown in Fig. 34.

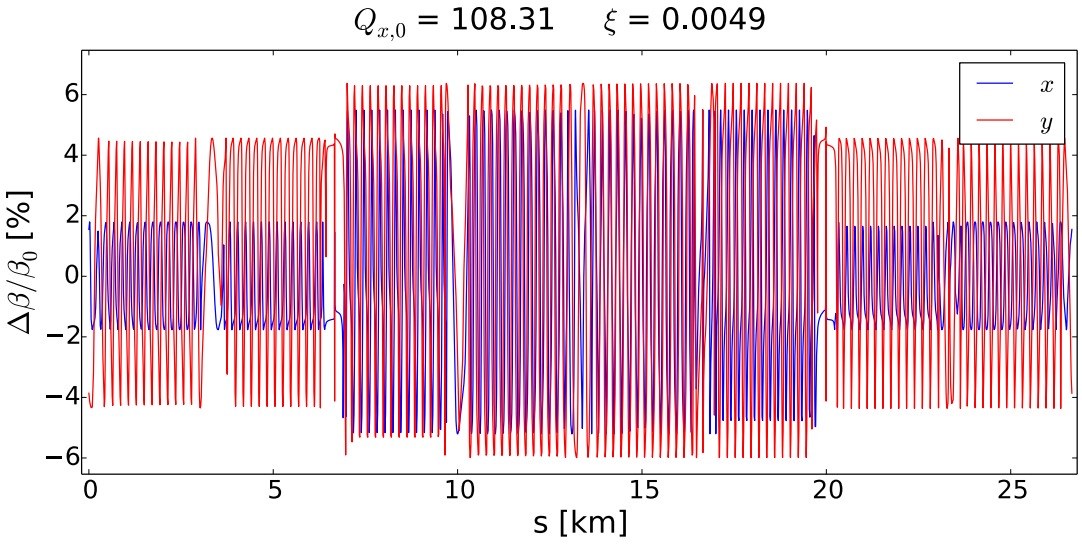

Figure 34: β-beating in the HL-LHC with two beam-beam interactions

One can notice that the beating has the same properties as the FCC-hh : the maximum beating relatively to both planes is not in the same order of amplitude. There will be places where the larger beating is in the vertical plane and in return places in the horizontal one.

The difference of amplitude of the beating depending on either we are on the right or the left to an interaction point is clear here too. Finally, the beating is proportional to the beam-beam parameter ξ chosen for the simulation as in all the previous cases.

Let's take a closer look at the β-beating at both interaction points IP1 and IP5 (Fig. 35 and 36). As one can see, the difference of variation of the beating follows the same logic as for the FCC-hh previously explained with the three parts.

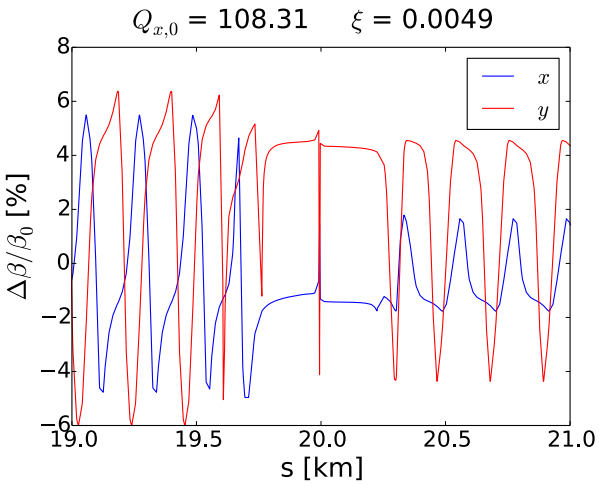

Figure 35: β-beating at IP1 due to beam-beam interactions at IP1 & IP5

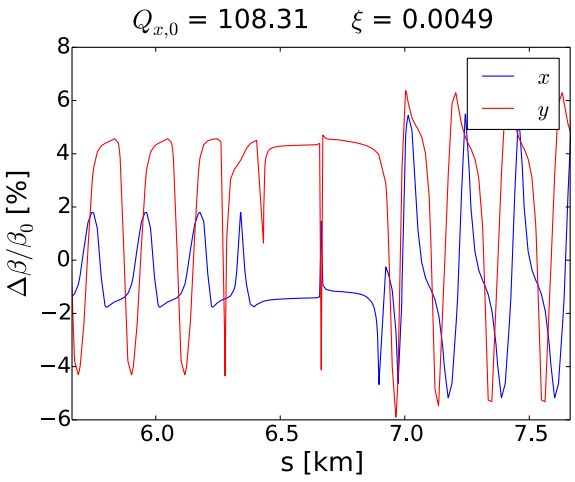

Figure 36: β-beating at IP5 due to beam-beam interactions at IP1 & IP5

The influence of the unperturbed horizontal tune $Q_{x,0}$ on the beating in the machine is not as evident as in the case with one beam-beam interaction here too. Indeed, not only the amplitude of the beating changes with respect to $Q_{x,0}$, but the ratio between the maximum of the beating of each part of an interaction point differs.

One can make the observation that the closer we are from $Q_{x,0} = 62.0$, the smaller is the ratio of the maximum between each side of the IP. And in return, the closer we are from $Q_{x,0} = 62.5$, the bigger is this ratio (Fig. 37 and 38) so that one can relate this to Eq. 14 as previously.

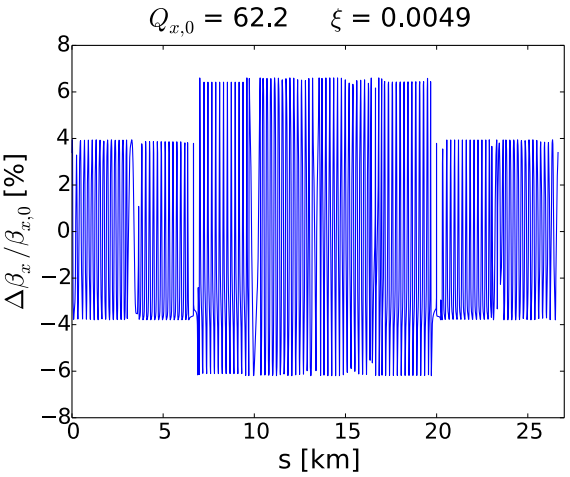

Figure 37: β-beating due to beam-beam interactions at IP1 & IP5

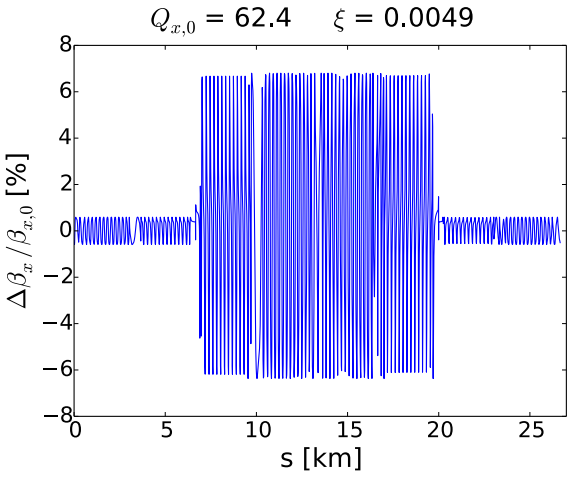

Figure 38: β-beating due to beam-beam interactions at IPA & IPG

Note that the shape of the β-beating at both IP's is approximately the same whatever the initial horizontal tune $Q_{x,0}$ is. The differences come mainly from the amplitude of the beating on each side of the interaction point like before.

As one can see on Fig. 39, the β-beating at the IP's with two beam-beam interactions is different from the one with one interaction (Fig. 4) and even from the FCC-hh with two beam-beam interactions (Fig. 28) for both planes. The β-functions increase at both IP's in the horizontal plane when the beam-beam parameter increases (like the FCC-hh with two beam-beam interactions) and decreases at both IP's in the vertical plane with respect to ξ (like the one beam-beam interaction case). We find again the symmetry between both interaction points for a given plane : the difference between each IP is in the order of 10^{-10}.

When a scan is performed on $Q_{x,0}$ for the β-beating at the IP's (Fig. 40), one can see that the latter is very similar at both interactions points IP1 and IP5 as previously : the difference between the two IP's is in the order of 10^{-10}, which shows one more time that the lattice is very symmetric even under the presence of two beam-beam interactions in the HL-LHC. We can also tell that the curve resembles to the one with one beam-beam interaction : the shape and the scales are similar. Notice that around $Q_{x,0} = 62.4$, the matching process didn't succeed perfectly and the complete convergence could be made. Indeed, the penalty function reached 10^{-10} instead of 10^{-12} like in all the other simulations, which leads to a small deviation in the value of the β-beating at the IP's compared to the other points in this graph.

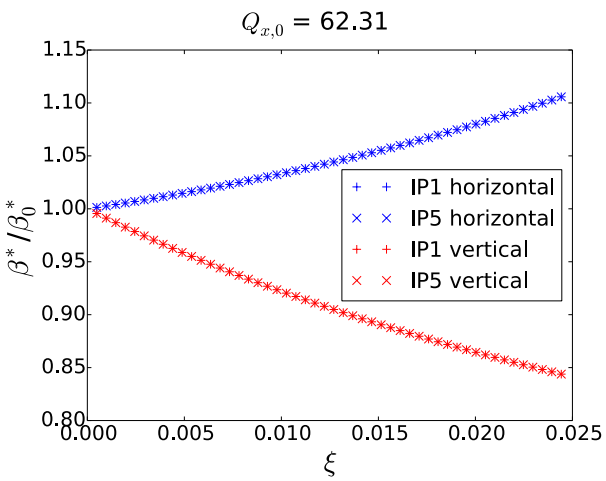

Figure 39: β-beating at the IP's due to beam-beam interactions at IP1 & IP5 as a function of ξ

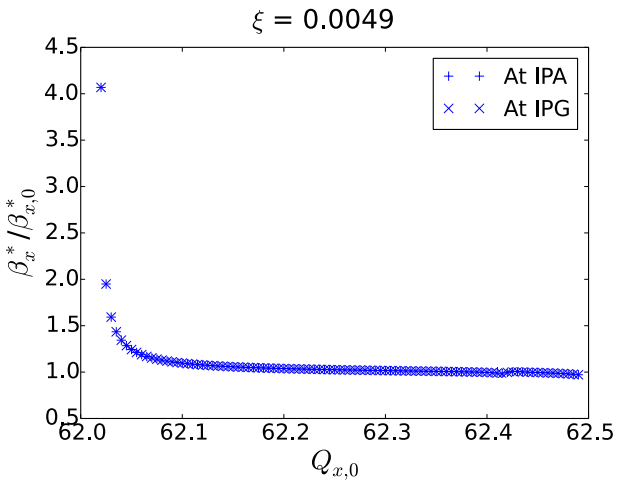

Figure 40: Horizontal β-beating at the IP's due to beam-beam interactions at IP1 & IP5 as a function of $Q_{x,0}$

Concerning the tune shift due to both beam-beam interactions (Fig. 41), one can mention a few points. First, the value of the tune shift is approximately twice bigger than in the case with one beam-beam interaction like before due to the linearity of the effects. Finally, the predominant change of tune occurs in the horizontal plane as in the case with one beam-beam interaction. The general behaviour remains however the same for one and two beam-beam interactions.

The incidence of the unperturbed horizontal tune $Q_{x,0}$ on the horizontal tune shift is given in Fig. 42. The curve has the same shape as the one with one beam-beam interaction, the size of the tune shift is however approximately the double of the beam-beam parameter

ξ when one is far from the resonances, which can be explained by the linearity of the effects.

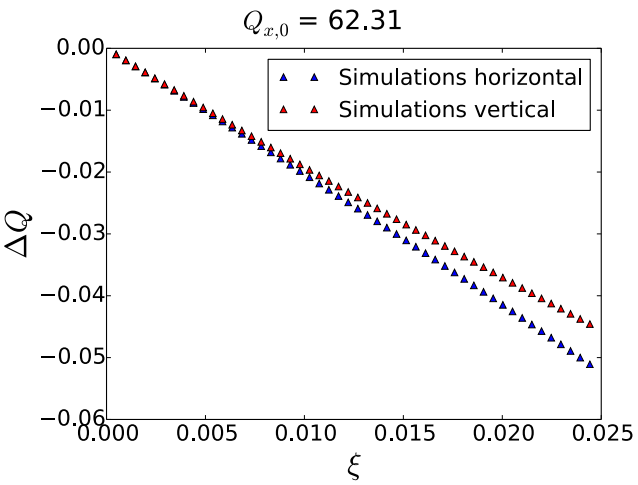

Figure 41: Tune-shift due to beam-beam interactions at IP1 & IP5 as a function of ξ

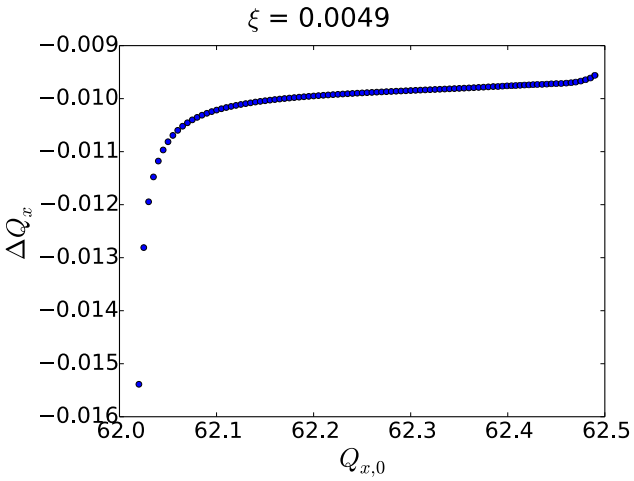

Figure 42: Horizontal tune shift due to beam-beam interactions at IP1 & IP5 as a function of $Q_{x,0}$

Concerning the maximum of the beating as a function of the beam-beam parameter ξ (Fig. 43), it has approximately the same shape as in the case with one beam-beam interaction. The particularity is that the maximum of the beating is more or less the same for small and large ξ but not really for intermediate ones ($\xi \approx 0.013$). The maximum is a little less than the double of the one with one beam-beam interaction ; the explanation is the same as previously for the FCC.

A scan on $Q_{x,0}$ for the maximum of the beating (Fig. 44) shows that the curve has the same shape as the one with one beam-beam interaction, the amplitude of the maximum is however approximately the double in the present case like before.

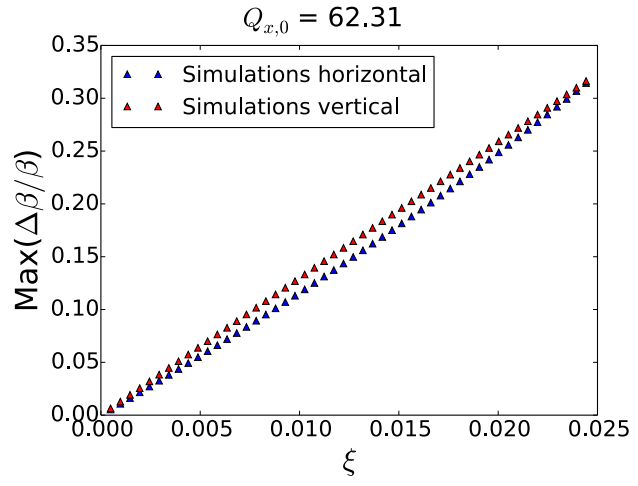

Figure 43: Maximum of the β-beating due to two beam-beam interactions at IP1 & IP5 as a function of ξ

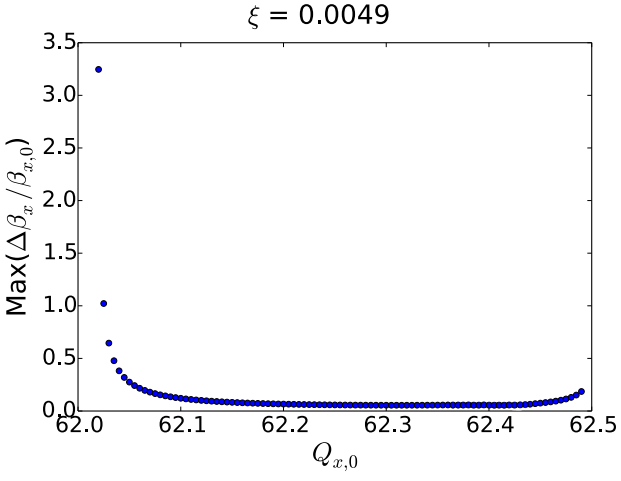

Figure 44: Maximum of horizontal β-beating due to two beam-beam interactions at IP1 & IP5 as a function of $Q_{x,0}$

5 Conclusion

In conclusion, this work permitted to show that MAD-X is a powerful tool that implements well the physics of the beam-beam interaction.

In the case of the FCC-hh and the HL-LHC, the analytical formulas concord with the evaluations of the optics functions using MAD-X except the maximum of the β-beating when performing a scan on the horizontal unperturbed tune $Q_{x,0}$.

It has been possible to see that the dynamics of the beams depends on the number of interaction points present in the machine such that it affects the β-function differently. In particular, the maximum of the β-beating could depend on the phase advance between the IP's and the amplitude of the beating could also change depending on the position in the accelerator.

The beam-beam parameter ξ and the initial tune Q_0 are other important parameters one should take into account when making collide two beams. More precisely, the beam-beam parameter indicates the amplitude of the perturbation given that the β-beating is proportional to it and Q_0 should be chosen far from resonances to avoid beam instabilities.

All the results are very symmetric with respect to the main interaction points chosen for both accelerators (IPA & IPG and IP1 & IP5). The lattice of the HL-LHC is however not perfectly symmetric compared to the FCC-hh whose lattice is fully symmetric.

References

[1] CERN Accelerator School - *Intermediate accelerator physics*, D. Brandt, CERN, Geneva, 2006.

[2] Wiedemann Helmut - *Particle Accelerator Physics*, Fourth Edition, Springer, 2015,

[3] Picture HL-LHC : http://www.nature.com/nature/journal/v448/n7151/full/nature06077.html

[4] Wu Chao Alexander, Tigner Maury - *Handbook of Accelerator Physics and Engineering*, World Scientific, 1999.

[5] Karl L. Brown - *A First- and Second-Order Matrix Theory for the Design of Beam Transport Systems and Charged Particle Spectrometers*, Slanford Linear Accelerator Center, Stanford, 1982.

[6] Iselin F. Christophe - *The MAD Program, Physical Methods Manual*, CERN, Geneva, 1994.

[7] De Maria Ricardo, Schmidt Frank and Skowronski Piotr Krzysztof - *Advances in matching with MAD-X*, CERN, Geneva.

[8] Lourakis Manolis I. A. - *A Brief Description of the Levenberg-Marquardt Algorithm*, FORTH, Crete, Greece, 2005.

6 Appendix

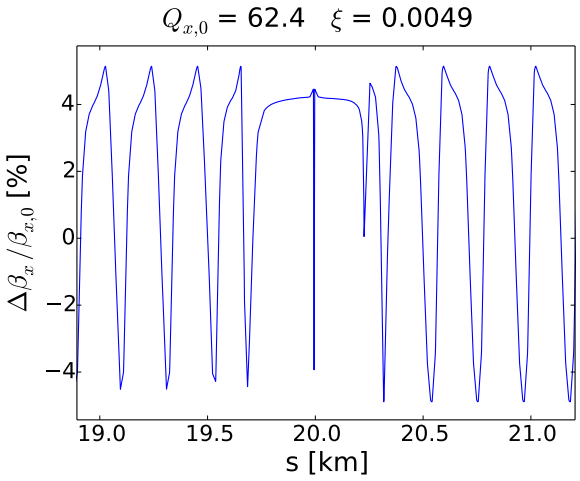

Figure 45: β-beating at IP1 due to beam-beam interaction placed at IP1

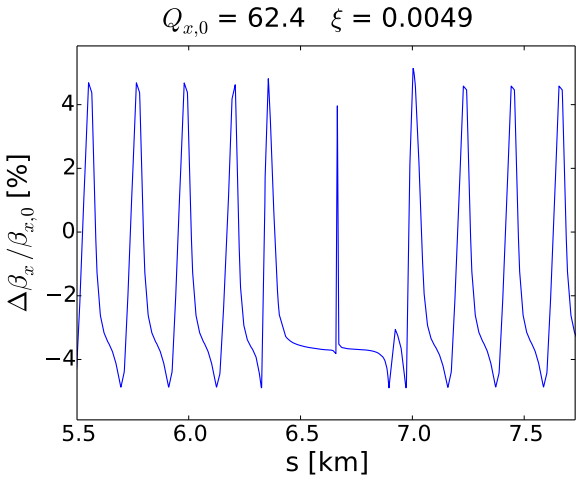

Figure 46: β-beating at IP5 due to beam-beam interaction placed at IP1